Supplementary Information.
Neural coding of binary mixtures in a structurally related odorant pair

Georgina Cruz & Graeme Lowe*,
Monell Chemical Senses Center,
Philadelphia, Pennsylvania 19104-3308
U.S.A.

§ 1. Calibration of odorant vapor concentration vs. liquid dilution

Glomerular dose-response relations of the odorants EG and MIEG were measured by varying their vapor concentrations using a liquid dilution olfactometer. The liquid dilution ratio of odorant to solvent (in our case mineral oil) may not be linearly related to vapor concentration due to deviations from ideal solution behavior[1,2]. To avoid non-linear distortion of dose-response relations, we used a photoionization detector (PID) to extract proportional measures of vapor concentration (Fig. S1).

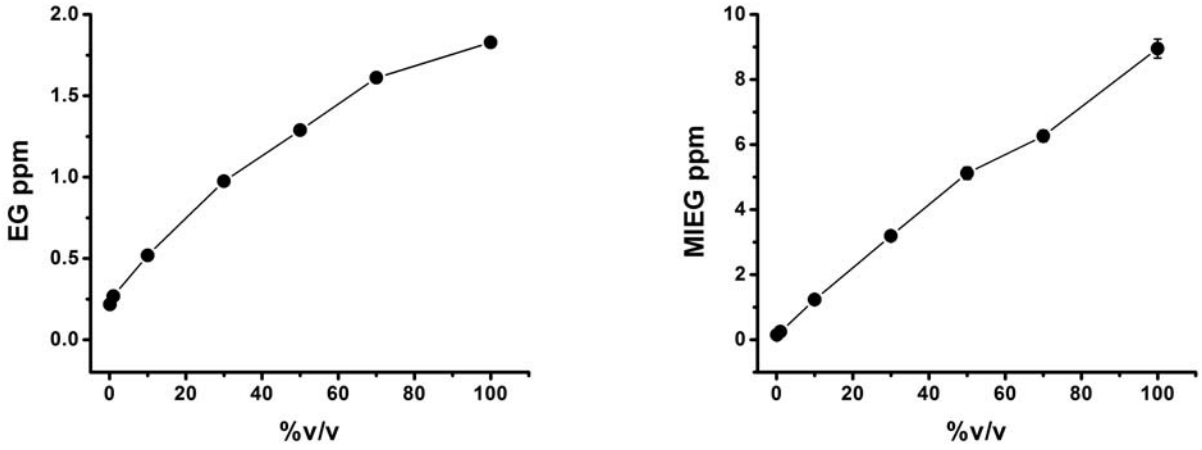

Figure S1. Plots of measured olfactometer delivered vapor concentrations of EG (left) and MIEG (right) vs. odorant liquid dilution. The ordinates of each data point represent the average of odorant concentrations measured at the olfactometer output nozzle by the PID in nominal (uncorrected) units of ppm, and the abscissa the liquid phase concentration in the olfactometer reservoir (% v/v liquid dilution in mineral oil). The plots reveal that liquid dilution did not scale linearly with vapor concentration, particularly for the less hydrophobic odorant EG. We used the nominal PID readings in all our analyses and model fitting.

§ 2. Model of the dose-response relation for competitive mixture interactions

To describe the binary mixture dose-response relations of glomeruli, we modeled three sequential steps in the odorant response: (1) competitive binding of a pair of odorant ligands (U and V) to a single binding site on an olfactory receptor; (2) single step activation of the receptor ligand complex; (3) cooperative saturable activation of the olfactory sensory neurons (OSNs) via the transduction cascade, leading to spike generation and transmitter release in presynaptic terminals.

For the first two steps, we followed the kinetic model of Rospars et al., (2008)[3]. Using their notation for convenience, the kinetic scheme for two odorants U and V competitively binding to receptor R, with independent activation is:

$$\begin{aligned} \mathrm{R} + \mathrm{U} &\underset{k_{-1\mathrm{U}}}{\overset{k_{1\mathrm{U}}}{\rightleftharpoons}} \mathrm{R.U} \underset{k_{-2\mathrm{U}}}{\overset{k_{2\mathrm{U}}}{\rightleftharpoons}} (\mathrm{R.U})^* \\ \mathrm{R} + \mathrm{V} &\underset{k_{-1\mathrm{V}}}{\overset{k_{1\mathrm{V}}}{\rightleftharpoons}} \mathrm{R.V} \underset{k_{-2\mathrm{V}}}{\overset{k_{2\mathrm{V}}}{\rightleftharpoons}} (\mathrm{R.V})^* \end{aligned} \qquad \text{..... (S1)}$$

with kinetic equations:

$$\begin{aligned} \frac{d[\mathrm{R}]}{dt} &= k_{-1\mathrm{U}}[\mathrm{R.U}] - k_{1\mathrm{U}}[\mathrm{R}][\mathrm{U}] + k_{-1\mathrm{V}}[\mathrm{R.V}] - k_{1\mathrm{V}}[\mathrm{R}][\mathrm{V}] \\ \frac{d[\mathrm{R.U}]}{dt} &= k_{1\mathrm{U}}[\mathrm{R}][\mathrm{U}] - k_{-1\mathrm{U}}[\mathrm{R.U}] = -\frac{d[\mathrm{U}]}{dt} \\ \frac{d[\mathrm{R.V}]}{dt} &= k_{1\mathrm{V}}[\mathrm{R}][\mathrm{V}] - k_{-1\mathrm{V}}[\mathrm{R.V}] = -\frac{d[\mathrm{V}]}{dt} \\ \frac{d[\mathrm{R.U}^*]}{dt} &= k_{2\mathrm{U}}[\mathrm{R.U}] - k_{-2\mathrm{U}}[\mathrm{R.U}^*] \\ \frac{d[\mathrm{R.V}^*]}{dt} &= k_{2\mathrm{V}}[\mathrm{R.V}] - k_{-2\mathrm{V}}[\mathrm{R.V}^*] \end{aligned} \qquad \text{..... (S2)}$$

We assume during the odor response that the reactions are at equilibrium, set all rates to zero, and define equilibrium constants:

$$K_{1U} = \frac{k_{-1U}}{k_{1U}},\ K_{2U} = \frac{k_{-2U}}{k_{2U}},\ K_{1V} = \frac{k_{-1V}}{k_{1V}},\ K_{2V} = \frac{k_{-2V}}{k_{2V}} \quad \text{..... (S3)}$$

From Eqn (S2) we obtain:

$$\begin{aligned} [\mathrm{R}]U &= K_{1U}[\mathrm{R.U}],\ [\mathrm{R}]V = K_{1V}[\mathrm{R.V}] \\ [\mathrm{R.U}^*] &= \frac{[\mathrm{R.U}]}{K_{2U}}, \quad [\mathrm{R.V}^*] = \frac{[\mathrm{R.V}]}{K_{2V}} \end{aligned} \quad \text{..... (S4)}$$

where $U = [\mathrm{U}]$, $V = [\mathrm{V}]$, are odorant concentrations, and from conservation of receptors, R_0:

$$R_0 = [\mathrm{R}] + [\mathrm{R.U}] + [\mathrm{R.V}] + [\mathrm{R.U}^*] + [\mathrm{R.V}^*] \quad \text{..... (S5)}$$

Eqns (S4) and (S5) lead to an expression for total concentration of activated state R*:

$$R^*(U,V) = \frac{R^*_{\mathrm{MU}} \frac{U}{K_{\mathrm{U}}} + R^*_{\mathrm{MV}} \frac{V}{K_{\mathrm{V}}}}{1 + \frac{U}{K_{\mathrm{U}}} + \frac{V}{K_{\mathrm{V}}}} \quad \text{..... (S6)}$$

where:

$$\begin{aligned} R^*_{\mathrm{MU}} &= \frac{R_0}{1 + K_{2U}},\ R^*_{\mathrm{MV}} = \frac{R_0}{1 + K_{2V}} \\ K_{\mathrm{U}} &= \frac{K_{1U}K_{2U}}{1 + K_{2U}},\ K_{\mathrm{V}} = \frac{K_{1V}K_{2V}}{1 + K_{2V}} \end{aligned} \quad \text{..... (S7)}$$

Eqn (S6) is identical to Eqn (A12) of Rospars et al, (2008)[3]. It is a hyperbolic function of two concentration variables, describing saturable equilibrium binding and activation by both odorants without cooperativity. For the third step of the model we empirically model the OSN response by a cooperative function of R^*. We use a single variable Hill equation to describe activation and saturation or adaptation of the downstream steps (including the olfactory transduction cascade, spike generation, and transmitter release at OSN terminals as reported by the spH signal):

$$F_{2D}(U,V)=\frac{F_M}{1+\left[\frac{K^*_R}{R^*(U,V)}\right]^{n_H}}=\frac{F_M}{1+\left[\frac{K^*_R\left(1+\frac{U}{K_U}+\frac{V}{K_V}\right)}{R^*_{MU}\frac{U}{K_U}+R^*_{MV}\frac{V}{K_V}}\right]^{n_H}} \quad \text{..... (S8)}$$

$$=\frac{F_{max}}{1+\left[\frac{1+\frac{U}{K_U}+\frac{V}{K_V}}{\eta_U\frac{U}{K_U}+\eta_V\frac{V}{K_V}}\right]^{n_H}}$$

where the parameters are: n_H, Hill coefficient; F_M, maximal response; K^*_R ,activation constant; $(\eta_U, \eta_V) = (R^*_{MU}/K^*_R,\ R^*_{MV}/K^*_R)$ efficiencies of activation of transduction by each odorant, relative to activation constant K^*_R of the downstream steps. Eqn (S8) corresponds to Eqn (2) in the text.

§ 3. Dose-response model for a single odorant

In the particular case of a single odorant U, setting $V = 0$ reduces Eqn (S8) to:

$$F_{1D}(U)=F_{2D}(U,0)=\frac{F_{max}}{1+\frac{1}{\eta_U{}^n}\left[1+\frac{K_U}{U}\right]^{n_H}} \quad \text{..... (S9)}$$

which corresponds to Eqn (1) in the text. Substituting $U = K_U$ in (S9), we obtain:

$$F_2(K_U)=\frac{F_{max}}{1+\left(\frac{2}{\eta_U}\right)^{n_H}} \quad \text{..... (S10)}$$

showing that K_U will be the odorant concentration at which there is half maximal glomerular response, if $\eta_U = R^*_{MU}/K^*_R = 2$, i.e. if maximal receptor activation is twice the activation constant of the downstream steps. The saturating response for (S9) is:

$$F_{1D}(\infty)=\frac{F_{max}}{1+\frac{1}{\eta_U{}^{n_H}}} \quad \text{..... (S11)}$$

which is less than F_{max}, and will only approach F_{max} if $\eta_U \gg 1$, i.e. $R_{max}^* \gg K^*$ (very efficient activation of downstream steps). At low odorant concentration, when $K_U/U \gg 1$:

$$F_{1D}(U) \sim F_{max}\left(\frac{\eta_U}{K_U}\right)^{n_H} U^{n_H} \quad \text{..... (S12)}$$

and the dose-response displays n_H^{th} order cooperativity near threshold.

§ 4. Cooperative mixture interactions

At higher odorant concentrations, hypoadditive mixture interactions occur due to saturation of receptor binding and activation, and saturation of downstream transduction steps of the OSNs. At lower odorant concentrations, the downstream steps may contribute either hypoadditivity ($n_H < 1$, negative cooperativity) or hyperadditivity ($n_H > 1$, positive cooperativity) to the mixture interaction. In order to accurately describe mixture interactions, it is necessary to correctly incorporate cooperativity into the model. As a test of the consistency of our model, we asked whether we can describe cooperative mixture interaction in the trivial case of a mixture of a single odorant with an equal amount of itself, i.e. whether $F_{2D}(U,U) = F_{2D}(2U,0)$. This is clearly true for Eqn (S8), because:

$$F_{2D}(U,U) = \frac{F_M}{1+\frac{1}{\eta_U{}^n}\left[\frac{K_U}{2U}+1\right]^{n_H}} = F_{2D}(2U,0) \qquad \text{..... (S13)}$$

At low odorant concentrations, $U \ll K_U$, we have:

$$F_{2D}(U,U) = F_{2D}(2U,0) \sim \frac{2^{n_H}\eta_U{}^{n_H}F_M}{K_U{}^{n_H}}U^{n_H} \sim 2^{n_H}F_{2D}(U,0) \qquad \text{..... (S14)}$$

which means that near threshold, if an equal amount of odorant is added to itself, the response is scaled 2^{n_H} fold by cooperativity.

In their analysis of binary mixture interactions, Rospars et al. (2008) modeled cooperativity by manually attaching a Hill coefficient, n_H, to each term in the numerator and denominator of Eqn (S6), and wrote the following formula (their Eqn (A13)):

$$F_{2DR}(U,V) = \frac{F_{MU}\left(\frac{U}{K_U}\right)^{n_H} + F_{MV}\left(\frac{V}{K_V}\right)^{n_H}}{1+\left(\frac{U}{K_U}\right)^{n_H}+\left(\frac{V}{K_V}\right)^{n_H}} \qquad \text{..... (S15)}$$

However, this model is unphysical because it fails the self-mixture test:

$$F_{2DR}(U,U)=\frac{2F_{\mathrm{MU}}\left(\frac{U}{K_{\mathrm{U}}}\right)^{n_{\mathrm{H}}}}{1+2\left(\frac{U}{K_{\mathrm{U}}}\right)^{n_{\mathrm{H}}}}\neq\frac{F_{\mathrm{MU}}\left(\frac{2U}{K_{\mathrm{U}}}\right)^{n_{\mathrm{H}}}}{1+\left(\frac{2U}{K_{\mathrm{U}}}\right)^{n_{\mathrm{H}}}}=F_{2DR}(2U,0) \quad \text{..... (S16)}$$

The two sides of Eqn (S16) are only equal under the special condition $n_{\mathrm{H}} = 1$, corresponding to a transduction cascade without cooperativity. The inconsistency of the model is clear at low odorant concentrations:

$$F_{2DR}(U,U)\sim 2F_{\mathrm{MU}}\left(\frac{U}{K_{\mathrm{U}}}\right)^{n_{\mathrm{H}}}\neq 2^{n_{\mathrm{H}}}F_{\mathrm{MU}}\left(\frac{U}{K_{\mathrm{U}}}\right)^{n_{\mathrm{H}}}=F_{2DR}(2U,0) \quad \text{..... (S17)}$$

i.e. the response to doubling odorant concentration is scaled cooperatively by a factor of $2^{n_{\mathrm{H}}}$, whereas the response to mixing an odorant with an equal quantity of itself is scaled additively by only a factor of 2. In general, mixture interactions in Eqn (S15) must always be hypoadditive:

$$\begin{aligned}F_{2DR}(U,V)&=\frac{F_{\mathrm{MU}}\left(\frac{U}{K_{\mathrm{U}}}\right)^{n_{\mathrm{H}}}}{1+\left(\frac{U}{K_{\mathrm{U}}}\right)^{n_{\mathrm{H}}}+\left(\frac{V}{K_{\mathrm{V}}}\right)^{n_{\mathrm{H}}}}+\frac{F_{\mathrm{MV}}\left(\frac{V}{K_{\mathrm{V}}}\right)^{n_{\mathrm{H}}}}{1+\left(\frac{U}{K_{\mathrm{U}}}\right)^{n}+\left(\frac{V}{K_{\mathrm{V}}}\right)^{n_{\mathrm{H}}}}\\&\leq\frac{F_{\mathrm{MU}}\left(\frac{U}{K_{\mathrm{U}}}\right)^{n_{\mathrm{H}}}}{1+\left(\frac{U}{K_{\mathrm{U}}}\right)^{n_{\mathrm{H}}}}+\frac{F_{\mathrm{MV}}\left(\frac{V}{K_{\mathrm{V}}}\right)^{n_{\mathrm{H}}}}{1+\left(\frac{V}{K_{\mathrm{V}}}\right)^{n_{\mathrm{H}}}}=F_{2DR}(U,0)+F_{2DR}(0,V)\end{aligned} \quad \text{..... (S24)}$$

i.e. $R_{\mathrm{MI}} \leq 1$, and Eqn (S15) could never model any hyperadditive mixture interaction.

The 2D surfaces described by Eqns (S8) and (S15) differ profoundly in their shapes over the lower halves of sigmoidal dose-response relations. We suggest that inferences regarding the existence of competitive vs. non-competitive mixture interactions based on Eqn (S15) may need revision.

§ 5. Modeling competitive antagonism

Although we did not observe it in this study, competitive antagonism between odorants was previously reported[4], and it can be easily accommodated as a special case of the competitive agonist model of binary mixture interaction by assuming that one of the two odorants binds and occupies the same receptor site as the other odorant, but does not activate the receptor.

Consider, for example, a situation in which the second odorant V antagonizes the response to the first odorant U. In Eqn (S1), we let the forward activation rate $k_{2V} \rightarrow 0$, so that in Eqn (S3) $K_{2V} \rightarrow \infty$, and in Eqn (S7) $R^*_{MV} \rightarrow 0$, and $K_V \rightarrow K1_V$. The concentration of activated ligand-receptor complex in Eqn (S6) then reduces to:

$$R^*(U,V) = \frac{R^*_{MU}\dfrac{U}{K_U}}{1+\dfrac{U}{K_U}+\dfrac{V}{K_{1V}}} \qquad \text{..... (S25)}$$

and the antagonized mixture response is modeled by the formula:

$$F_{2D}(U,V) = \frac{F_M}{1+\left[\dfrac{K^*_R}{R^*(U,V)}\right]^{n_H}} = \frac{F_M}{1+\left[\dfrac{K^*_R\left(1+\dfrac{U}{K_U}+\dfrac{V}{K_{1V}}\right)}{R^*_{MU}\dfrac{U}{K_U}}\right]^{n_H}} = \frac{F_{max}}{1+\left[\dfrac{1+\dfrac{U}{K_U}+\dfrac{V}{K_{1V}}}{\eta_U\dfrac{U}{K_U}}\right]^{n_H}} \qquad \text{..... (S26)}$$

More generally, odorant V could partially antagonize (suppress) the response to odorant U if it competed for receptor occupancy, but only weakly activated the receptor. If there is a large difference in equilibrium constants, $K_{2V} \gg K_{2U}$, then $\alpha = R^*_{MV}/R^*_{MU} \ll 1$, and the addition of V would reduce the concentration of activated receptor state R*:

$$R^*(U,V) = R^*_{MU}\frac{\dfrac{U}{K_U}+\alpha\dfrac{V}{K_V}}{1+\dfrac{U}{K_U}+\dfrac{V}{K_V}} \qquad \text{..... (S27)}$$

because V adds a much larger term to the denominator than the numerator.

§ 6. Validation of 2D model fitting procedures

The 2D model equation (S8) was used to fit binary mixture dose-response data sets for odorants EG and MIEG, and estimate values of the parameters (F_{max}, K_{EG}, K_{MIEG}, n_H ,η_{EG}, η_{MIEG}). To test the ability of our least squares fitting procedure to estimate these parameters, we used the model to generate, for 4 representative glomeruli in reciprocal experiments, a total of 6 mock data sets by calculating $F = \Delta F/F_0$ values with known model parameters, and attempted to recover these parameters using our fitting procedure. Model parameters used were those obtained by data fitting, and calculated F values were modified by adding random Gaussian noise to simulate experimental error. Noise distributions were chosen with variance similar to those of measured dose-response relations (CV range 10 – 90 %).

	m1g2		**m1g6**		**m3g4**		**m4g3**	
	E+M	**M+E**	**E+M**	**M+E**	**E+M**	**M+E**	**E+M**	**M+E**
K_{EG} (mod)	0.49	0.71	0.96	0.40	0.65	0.43	0.64	0.46
K_{EG} (rec)	0.40–0.49	0.67– 0.80	0.94–1.43	0.40–0.48	0.29–0.70	0.32–0.67	0.43–0.64	0.28–0.57
F_{max} (mod)	1.04	1.12	0.95	1.36	0.97	0.56	0.91	0.60
F_{max} (rec)	0.91–1.39	1.08–1.21	0.87–1.23	0.88–1.56	0.68–1.37	0.20–0.59	0.41–1.57	0.53–1.06
n_H (mod)	2.01	2.12	1.51	0.40	1.12	1.47	1.32	1.10
n_H (rec)	1.83–2.11	1.99–2.31	1.39–1.65	0.35–0.40	1.09–1.24	1.34–1.54	1.22–1.53	1.01–1.13
η_{EG} (mod)	4.17	4.47	4.85	5.46	3.23	2.04	3.27	2.52
η_{EG} (rec)	3.92–5.63	3.78–4.76	3.73–8.19	5.27–7.74	1.80–3.27	1.95–2.71	2.32–6.28	2.61–5.02
η_{MIEG} (mod)	1.62	1.45	2.42	1.48	2.39	1.25	2.26	1.74
η_{MIEG} (rec)	1.47–1.72	1.42–1.60	2.34–2.68	1.49–1.62	1.32–2.40	1.06–1.43	1.64–2.52	1.54–2.06

Table ST1. Summary of model input (mod) and range of recovered output (rec) values of 5 model parameters for reciprocal mock experiments, where either MIEG was added to EG (E+M), or EG added to MIEG (M+E).

Glomerulus	Range of added noise (± % CV)	synthetic data sets paired sample t-test, P-values					
		data1	data2	data3	data4	data5	data6
EG+MIEG							
m1g2	10 – 40	0.73	0.91	0.30	0.31	0.51	0.49
m1g6	10 – 50	0.35	0.74	0.86	0.26	0.54	0.89
m3g4	10 – 30	0.24	0.22	0.42	0.51	0.84	0.24
m4g3	10 – 90	1.00	0.74	0.37	0.67	0.46	0.50
MIEG+EG							
m1g2	10 – 50	0.55	0.26	0.97	0.24	0.83	0.26
m1g6	10 – 90	0.23	0.41	0.42	0.56	0.45	0.27
m3g4	10 – 60	0.43	0.66	0.58	0.84	0.37	0.90
m4g3	10 – 50	0.67	0.82	0.85	0.37	0.29	0.37

Table ST2. Summary of P-values obtained from statistical tests comparing model input and recovered output values of 6 model parameter sets. Groups of recovered values satisfied Kolmogorov-Smirnov tests of normality (P = 0.75–1.0, n = 6). Therefore, comparisons were performed with paired t-tests (n = 6 comparisons per data set for each reciprocal experiment). In all cases P > 0.05 indicating no significant difference between input and recovered values, thus validating our fitting procedures.

§ 7. 2D model parameters obtained from pure odorant dose response data.

In Figures 5f, 5g, we compared measured glomerular responses with those predicted from 2D models, to test how well the model described a situation of complete odorant overlap in the epithelium (C-model, Eqn (S8)) and no odorant overlap (AB-model, chromatographic separation). Values of model parameters for glomeruli were derived by performing 2D fits to pure odorant dose-responses as joint data sets (EG alone plus MIEG alone). The values obtained were similar to those obtained by fitting 1D models to the dose-responses, or by fitting the 2D C-model to the full data sets including mixture responses (c.f. Table ST3, vs. Tables 1 and 2 in text).

	EG			MIEG		
	range	median	mean ± SD	range	median	mean ± SD
K	0.18 – 0.83	0.51	0.51 ± 0.19	0.18 – 1.32	0.73	0.74 ± 0.31
F_{max}	0.44 – 1.88	0.87	0.96 ± 0.41	same as EG		
n	2.03 – 5.46	3.42	3.58 ± 0.99			
η	1.68 – 3.26	2.04	2.14 ± 0.40	1.76 – 2.99	2.22	2.23 ± 0.32
RSS	0.12 – 0.98	0.42	0.47 ± 0.26	same as EG		

Table ST3. Variation in model parameters obtained by fitting pure EG and MIEG dose-response relations of 15 individual glomeruli to a competitive binding model equation (Eqn (2) in text) (data from 4 mice). RSS (residual sum of squares) is the fitting error.

§ 8. Chromatographic effects on mixture interactions

The OSN response to an odorant mixture is determined by the receptor binding interactions of mixture components. These interactions will depend on the relative concentrations of mixture components at the binding sites. However, concentration ratios are not necessarily constant for all OSNs in the olfactory epithelium. Mixture components with different physicochemical properties (e.g. polarity, hydrophobicity) may be differentially adsorbed by the olfactory mucosa and experience spatial separation by a mechanism analogous to gas chromatography[5-7]. This process is predicted to favor mixture interactions between odorant pairs with similar properties that are adsorbed in more overlapping areas of mucosa, and to reduce interactions between odorant pairs with different properties that are adsorbed in more spatially segregated areas[8,9]. For example, polar odorants would be strongly adsorbed early in the inspiratory airstream, and this may reduce their concentrations at downstream receptors sites relative to hydrophobic odorants. Chromatographic effects could impact glomerular responses to mixtures because glomeruli integrate convergent inputs from OSNs dispersed across broad areas of olfactory epithelium[10,11].

We searched for chromatographic effects on mixture interactions between EG and MIEG by fitting our dose-response data to a simple model of odorant separation. The glomerular response was divided into three terms, representing input from receptors activated only by EG, only by MIEG, and by both EG and MIEG:

$$F = A.F_{2D}(U,0) + B.F_{2D}(0,V) + C.F_{2D}(U,V) \quad \text{.....} \quad \text{(S28)}$$

where coefficients of the first two terms (A and B), represent fractional inputs from receptors stimulated only by EG, or only by MIEG respectively, and of the third term ($C = 1 - A - B$) the

fractional input from overlap receptors stimulated by both EG and MIEG. This model makes several simplifying assumptions: (i) uniform receptor density in areas exposed to odorants, (ii) uniform distribution of odorants in areas of adsorption, and (iii) discrete adsorption areas (Fig. S2a). We compared model fits to mixture response data for two limiting cases: (i) complete odorant separation, with only first two terms in Eqn (S28) ('AB'-model, $C = 0$) and (ii) complete odorant overlap with only the third term ('C'-model, $A = B = 0$, i.e. Eqn (2)). For all glomeruli, we found that fit errors were larger for complete separation (global residual sum-of-squares, RSS = 3.31 ± 0.45, $n = 30$) than for complete overlap (RSS = 2.02 ± 0.31, $n = 30$) (Mann-Whitney test, $P < 0.05$). Thus mixture responses were better predicted by the C-model (overlap) than the AB-model (separation). To highlight this, first we fitted 2D models to single odorant dose response data for EG or MIEG taken together, and then compared mixture responses predicted from these fits to observed mixture responses. Both the C- and AB-models yielded good fits to single odorant responses (Fig. S2f). In contrast, the mixture responses were well predicted from single odorant fits in the C-model (Figs. S2b, d), but poorly predicted in the AB-model (Figs. S2c, e). Thus, our mixture responses were consistent with non-linear competitive interaction of completely overlapping odorants, and not with additive combination of responses to chromatographically separated odorants. We also fitted a general model with partial odorant separation, i.e. $A + B < 1$, with 3 terms in Eqn (S28). This yielded a slightly smaller mean error (RSS = 1.879 ± 0.316) for a subset of glomeruli. However, the difference was not statistically significant (Mann-Whitney test, $P = 0.32$).

At this stage we cannot rule out the possibility of chromatographic effects in EG and MIEG responses because subtle differences in odorant adsorption patterns would not be possible to resolve in this model. Our modeling of odorant separation was performed more as a conceptual exercise than a rigorous test of the chromatographic hypothesis. More realistic models will need to account for continuous adsorption gradients, and the complexities of nasal anatomy, airflow patterns and glomerulus-specific zonal expression of olfactory receptors.

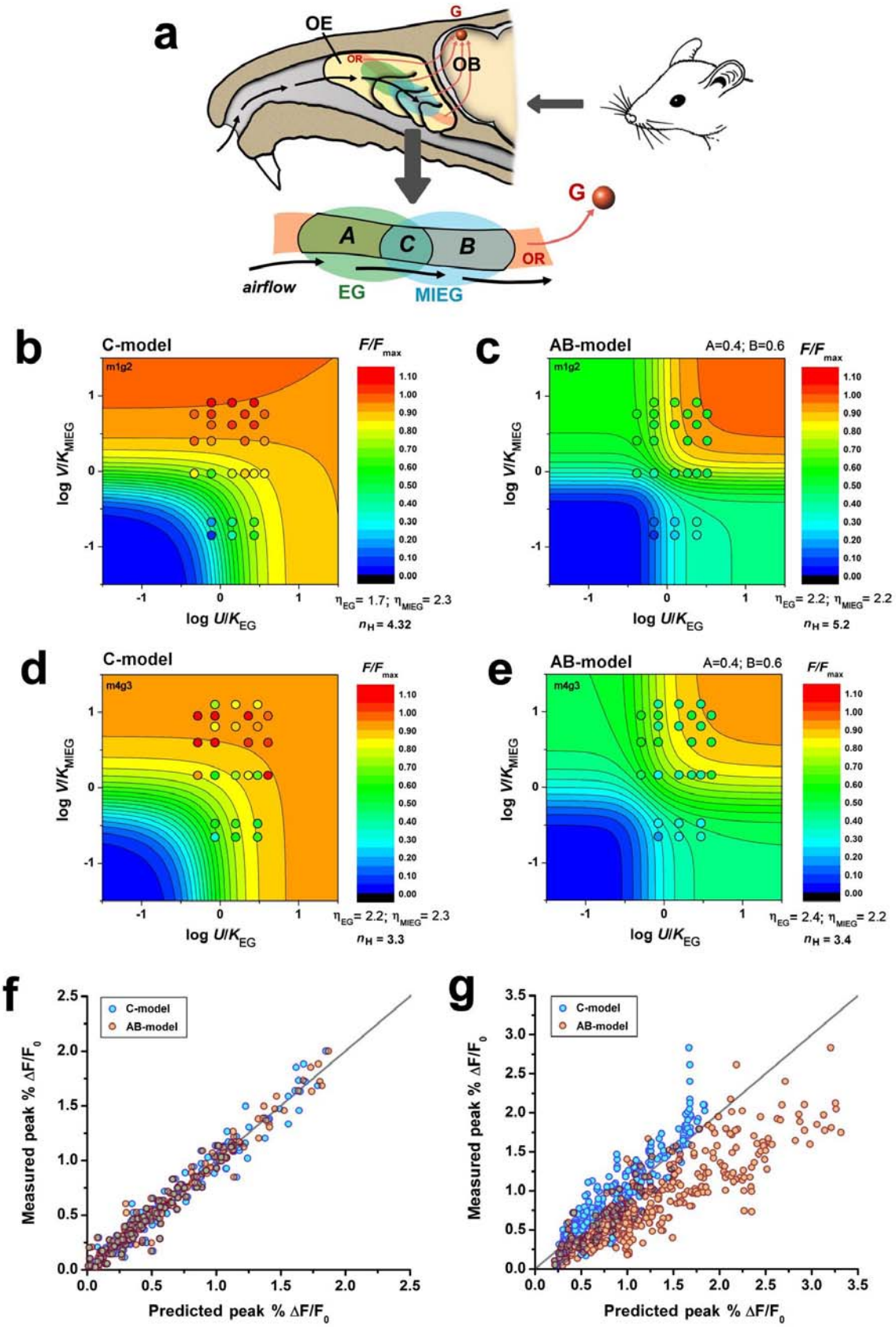
a
OE
G
OR
OB
G
A
C
B
OR
airflow
EG
MIEG
b
C-model
m1g2
F/F max
log V/K MIEG
log U/K EG
η EG= 1.7; η MIEG= 2.3
n H = 4.32
c
AB-model
A=0.4; B=0.6
m1g2
η EG= 2.2; η MIEG= 2.2
n H = 5.2
d
C-model
m4g3
η EG= 2.2; η MIEG= 2.3
n H = 3.3
e
AB-model
A=0.4; B=0.6
m4g3
η EG= 2.4; η MIEG= 2.2
n H = 3.4
f
C-model
AB-model
Measured peak % ΔF/F 0
Predicted peak % ΔF/F 0
g
C-model
AB-model
Measured peak % ΔF/F 0
Predicted peak % ΔF/F 0

Figure S2. Quality of fit of the competitive model of mixture interactions is reduced by chromatographic separation of EG and MIEG. **a.** Schematic of a simplified model of spatial separation of EG and MIEG in the olfactory mucosa. Inhaled airflow (arrows) delivers EG and MIEG to the olfactory epithelium (OE), where they partition across two regions (green and blue, respectively) that overlap the expression zone (orange) of an olfactory receptor (OR) with convergent projections to a glomerulus (G) in the dorsal olfactory bulb (OB). Relative areas of odorant adsorption along the OR expression zone are represented in the model (Eqn (4)) by three coefficients: A (only EG adsorbed), B (only MIEG adsorbed), and $C = 1 - (A+B)$ (overlap area with both EG and MIEG adsorbed). **b–e.** Color plots of measured $\Delta F/F_0$ responses (circles, normalized to fitted F_{max}) from two glomeruli (m1g2 in **b, c**; m4g3 in **d, e**) as functions of U = [EG] and V = [MIEG], with log concentration scales normalized to receptor binding and activation constants K_{EG} and K_{MIEG}. Underlying contour plots represent model surfaces obtained by fitting Eqn (4) to non-mixture data (single odorant dose-response) either for fully overlapped adsorption (**b, d:** C-model, $A = B = 0$), or for complete chromatographic separation (**c, e:** AB-model, $C = 0$). Contours have same color scale as measured points, so color differences between circle fills and background show differences between measured mixture responses and model predictions from the single odorant responses. **f.** Plot of 240 measured single odorant responses (EG or MIEG,15 glomeruli, range of concentrations) vs. corresponding responses predicted from model fits to non-mixture data, for C-model (blue circles) and AB-model (orange circles). **g.** Plot of 450 measured mixture responses (EG and MIEG, 15 glomeruli, range of concentrations) vs. corresponding responses predicted from model fits to non-mixture (single odorant) data, for C-model (blue circles) and AB-model (orange circles).

Reference List

1. Oka,Y. *et al.* Odorant receptor map in the mouse olfactory bulb: in vivo sensitivity and specificity of receptor-defined glomeruli. *Neuron* **52**, 857-869 (2006).

2. Cometto-Muniz,J.E., Cain,W.S. & Abraham,M.H. Quantification of chemical vapors in chemosensory research. *Chem Senses* **28**, 467-477 (2003).

3. Rospars,J.P., Lansky,P., Chaput,M. & Duchamp-Viret,P. Competitive and noncompetitive odorant interactions in the early neural coding of odorant mixtures. *J. Neurosci.* **28**, 2659-2666 (2008).

4. Oka,Y., Omura,M., Kataoka,H. & Touhara,K. Olfactory receptor antagonism between odorants. *EMBO J.* **23**, 120-126 (2004).

5. Mozell,M.M. & Jagodowicz,M. Chromatographic separation of odorants by the nose: retention times measured across in vivo olfactory mucosa. *Science* **181**, 1247-1249 (1973).

6. Mozell,M.M. Evidence for sorption as a mechanism of the olfactory analysis of vapours. *Nature* **203**, 1181-1182 (1964).

7. Mozell,M.M. Olfactory Discrimination: Electrophysiological Spatiotemporal Basis. *Science* **143**, 1336-1337 (1964).

8. Bell,G.A., Laing,D.G. & Panhuber,H. Odour mixture suppression: evidence for a peripheral mechanism in human and rat. *Brain Res* **426**, 8-18 (1987).

9. Laing,D.G. Coding of chemosensory stimulus mixtures. *Ann. N. Y. Acad. Sci.* **510**, 61-66 (1987).

10. Miyamichi,K., Serizawa,S., Kimura,H.M. & Sakano,H. Continuous and overlapping expression domains of odorant receptor genes in the olfactory epithelium determine the dorsal/ventral positioning of glomeruli in the olfactory bulb. *J. Neurosci.* **25**, 3586-3592 (2005).

11. Ressler,K.J., Sullivan,S.L. & Buck,L.B. A zonal organization of odorant receptor gene expression in the olfactory epithelium. *Cell* **73**, 597-609 (1993).

12. Schoenfeld,T.A. & Cleland,T.A. The anatomical logic of smell. *Trends Neurosci.* **28**, 620-627 (2005).